ISSN 2682-681X (Paper), ISSN 2705-4241 (Online) | http://unilorinjoger.com | https://doi.org/10.63745/joger.2026.06.30.012

JOURNAL OF GEOMATICS AND ENVIRONMENTAL RESEARCH
www.unilorinjoger.com

RESEARCH ARTICLE

Geostatistical Modelling and Spatial Variability Analysis of Soil Macronutrients in the Federal Capital Territory, Nigeria, Using Soil Spectroscopy

Abdul Ibrahim*[1], Adelakun Isaac Gbiri [1], Rachael Olubunmi Ogunsola[2], Adesayo Titus Oduyemi[1], Michael Bako[3]

[1]Department of GIS and Cartography, Federal School of Survey, Oyo, Nigeria
[2]Department of Surveying and Geoinformatics, Federal School of Survey, Oyo, Nigeria
[3]Department of Surveying and Geoinformatics, Federal University of Technology, Minna, Nigeria.

*Corresponding author email: brawnabdulibrahim@fss-oyo.edu.ng

Abstract

Efficient soil nutrient management is increasingly critical in Nigeria's Federal Capital Territory (FCT), where rapid urbanization has strained agricultural productivity. This study evaluates the spatial distribution and heterogeneity of soil nitrogen (N), phosphorus (P), and potassium (K) using geostatistical modeling and soil spectroscopy. A total of 127 soil samples were collected from the plough layer (0–30 cm) using a GPS-guided sampling design. Nutrient concentrations were determined via spectroscopy, and the resulting data were modeled using semivariogram analysis and ordinary kriging interpolation to visualize distribution patterns across the territory. The results reveal strong spatial dependencies and significant nutrient deficiencies throughout the FCT. Specifically, 94% of the study area exhibited "low" to "very low" nitrogen levels, primarily concentrated in the Gwagwalada, Kwali, Bwari, and Abaji councils. Similarly, phosphorus and potassium levels were predominantly deficient, with moderate concentrations restricted to only 11% and 8% of the territory, respectively, largely within the Kuje Area Council. The high spatial variability observed underscores the inadequacy of traditional blanket fertilizer applications. These findings provide a robust geospatial framework for site-specific nutrient management (SSNM) and demonstrate the efficacy of integrating geostatistics with soil spectroscopy for regional agricultural planning and resource optimization.

ARTICLE HISTORY
Received: 20 May 2026
Accepted: 29 May 2026
Published: 30 May 2026

KEYWORDS
Geostatistics, Ordinary Kriging, Soil Spectroscopy, Spatial Architecture, Precision Agriculture, FCT.

Citation: Ibrahim A., Gbiri I. A., Ogunsola R.O., Oduyemi A.T., & Bako M. (2026). Geostatistical Modelling and Spatial Variability Analysis of Soil Macronutrients in the Federal Capital Territory, Nigeria, Using Soil Spectroscopy. *Journal of Geomatics and Environmental Research*, *9(1), Pp 148-161*

1. INTRODUCTION

The precise characterization of soil nutrient variability is fundamental to the advancement of precision agriculture and regional food security (Niharika *et al.,* 2025). Soil properties are inherently characterized by high degrees of spatial heterogeneity, driven by a complex interplay of pedogenic processes and anthropogenic influences (Qin *et al.,* 2026). In rapidly developing regions like the Federal Capital Territory (FCT), Nigeria, these natural variations are further complicated by shifting land-use patterns and intensive cultivation (Iwalaiye *et al.,* 2024). However, the lack of high-resolution, spatially explicit data regarding soil macronutrient status remains a significant barrier to sustainable land management (Aditya *et al.,* 2025).

The optimization of agricultural output is intrinsically linked to the availability of essential macronutrients, specifically Nitrogen (N), Phosphorus (P), and Potassium (K) (Khan *et al.,* 2023; Cao *et al.,* 2025). These elements form the critical NPK trio, governing plant metabolic processes and structural development (Zewide & Reta, 2021). Consequently, a precise determination of NPK spatial distribution is not merely beneficial but sacrosanct to modern agricultural production (Zheng *et al.,* 2022). However, soil properties are characterized by high degrees of spatial heterogeneity, meaning that point-based sampling, as seen in Zhang *et al.* (2024), without spatial modeling often provides an incomplete representation of the landscape.

To address these complexities, geostatistical techniques have emerged as a robust framework for quantifying and mapping the spatial architecture of soil properties. Unlike deterministic interpolation, geostatistics accounts for spatial autocorrelation, providing a more reliable estimation of unsampled locations. These methods have been successfully deployed globally, such as in the characterization of soil property variability in Colombia (Álvarez-Herrera *et al.,* 2025) and Geostatistical Analysis of Soil Reaction, Electrical Conductivity, and Organic Matter Content in Bangladesh (Islam *et al*., 2018). Regionally, geostatistics has been utilized to map Soil Exchangeable Basic Cations Along River Wudil Floodplain Kano (Khallah *et al.,* 2025).

Despite the proven efficacy of these techniques, there remains a notable paucity of recent, large-scale geostatistical assessments focused specifically on agricultural zones in the FCT; the closest is the Analysis of the Spatial Variability of Soil Nutrients using Geospatial Techniques for Improved Precision Agriculture Practices in Minna, Nigeria (Bako *et al.,* 2025). This study addresses this knowledge gap by employing semivariogram analysis and Ordinary Kriging to evaluate the spatial heterogeneity of NPK across the territory. The results aim to provide a data-driven foundation for site-specific nutrient management, bridging the gap between geospatial science and regional food security.

2. MATERIALS AND METHODS

2.1 The Study Area

The Federal Capital Territory (FCT) of Nigeria is situated within the North-Central geopolitical zone, geographically bounded by latitudes $8^0$15'00"N to $9^0$12'00"N and longitudes $6^0$27'00"E to $7^0$23'24"E (Figure 1). Occupying an approximate land area of 8,000 km^2, the territory is bordered by the states of Niger to the west and north, Kaduna to the northeast, Nassarawa to the east and southeast, and Kogi to the southwest (Adeiza *et al.,* 2023). The region is characterized by a Guinea Savanna vegetation complex, which plays a pivotal role in the local pedogenesis and nutrient cycling of the soil. Topographically, the FCT presents a varied landscape of undulating plains and prominent granitic hills, influencing the spatial distribution of runoff and mineral deposition. Agriculture remains the primary economic driver; however, the sector faces significant spatial pressure from rapid demographic expansion, with the population estimated to have reached approximately 3.56 million by 2023. The planned capital city, Abuja, serves as the central administrative hub, around which significant land-use and land-cover (LULC) transitions have occurred since the inception of the territory.

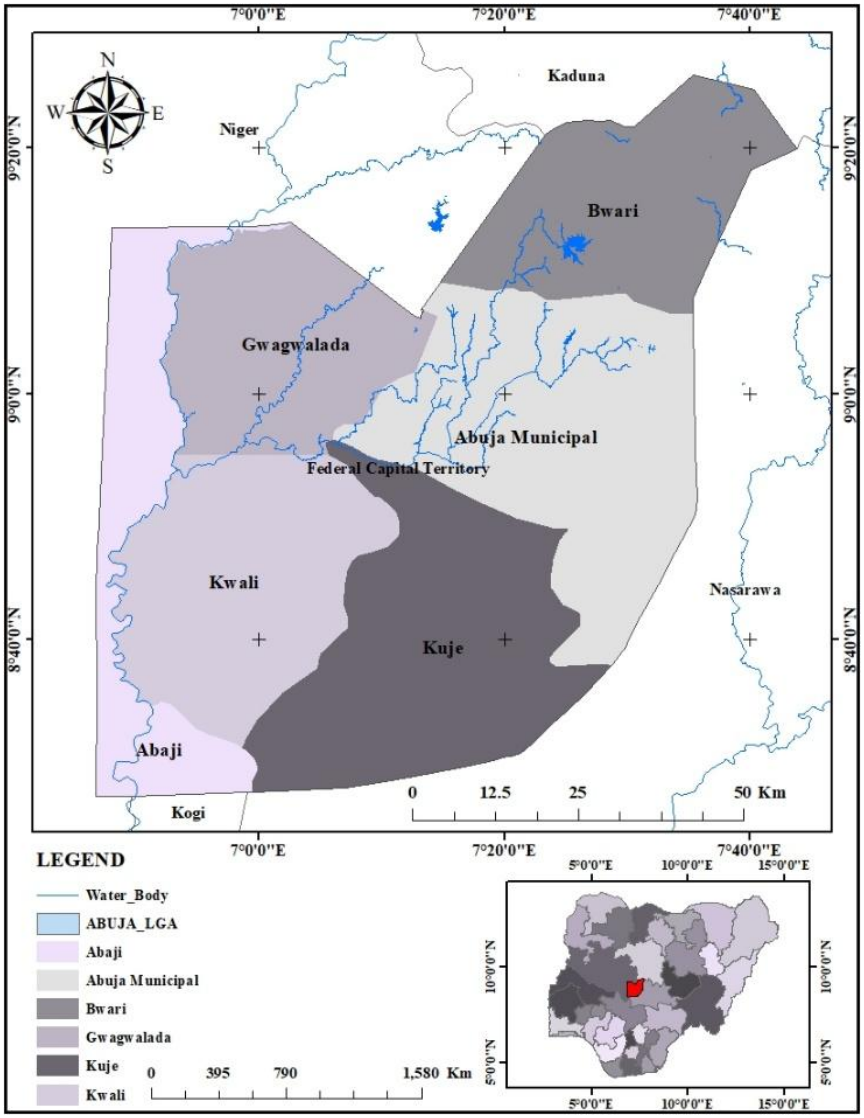

Figure 1. Study Area showing LGAs in Abuja FCT (source: Authors Lab, 2026)

2.2 Data Processing

The study utilized the spatial analytical capabilities of GIS to integrate thematic and positional datasets, leveraging location as a primary variable to extract complex patterns from soil nutrient data. A rigorous Exploratory Data Analysis was first conducted, including summary statistics, normality testing, and variogram analysis to characterize the statistical properties and spatial dependency of the NPK dataset. Subsequently, Ordinary Kriging was deployed as the core stochastic model to generate continuous prediction surfaces by fitting optimized mathematical models to empirical semivariograms (Ítalo *et al.,* 2026). This geostatistical approach was complemented by GIS operations such as attribute queries, proximity analysis, and spatial overlays, effectively converting discrete point observations into high-resolution information surfaces for a comprehensive evaluation of the soil architecture. The dataset for this study is summarized in Table 1, while Table 2 displays the soil samples and the coordinate points and Figure 2 shows the workflow diagram.

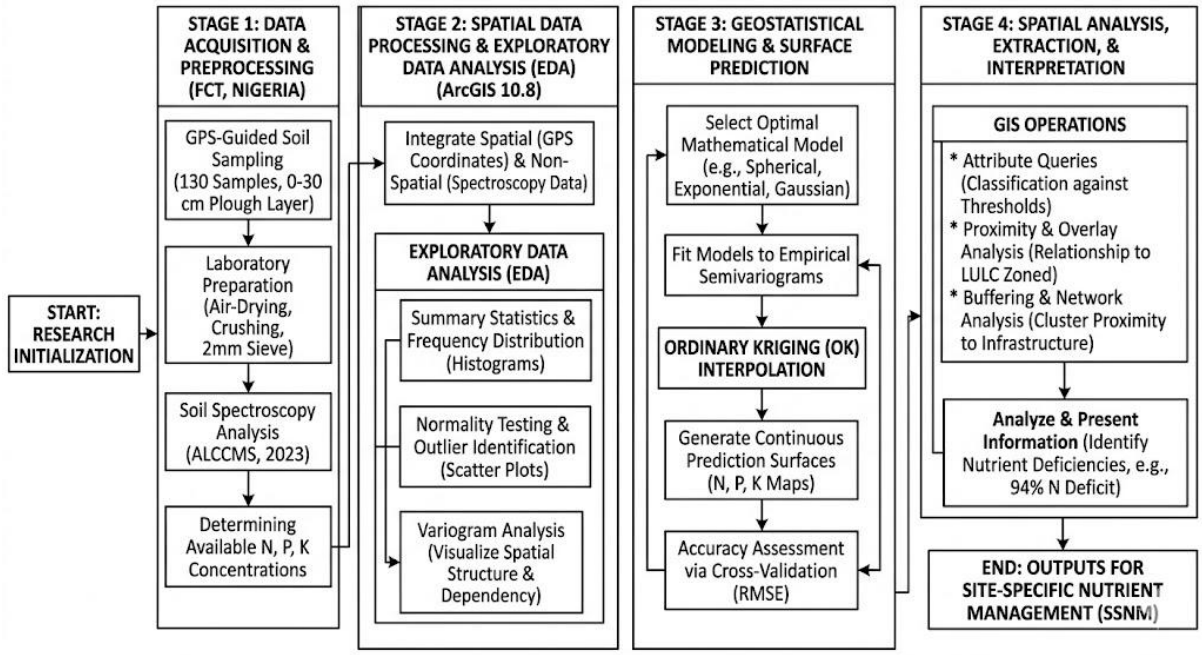

Figure 2. Methodological workflow for soil spectroscopy, spatial data processing, geostatistical modelling and surface prediction and spatial analysis, extraction and interpretation.

Table 1. Materials used for study

Category	Type	Description/Usage
Data Sample	Point Data	FCT Soil Survey Result used for geostatistical analytical modelling of soil NPK spatial distribution.
Software/Programs	ESRI ArcGIS, Microsoft Excel	Geospatial and Geostatistical analysis, Semivariogram, Kriging interpolation, and map production
Input data	CSV files, Shapefiles	Point sample data was instrumental for interpolation and administrative boundaries to show all local governments in FCT, combined with other layers.

Table 2: Soil samples and coordinate points

S/N	latitude	longitude	Textural class	SOC (%)	N(%)	P (mg/Kg)	K(cmol/Kg)
1.	8.455063	6.922012	Sand	0.2767	0.0314	19.79719467	0.203745
2.	8.455260	6.922034	Loamy Sand	0.2425	0.0267	16.62252167	0.162177
3.	8.472098	6.933888	Sand	0.2943	0.0311	18.95911033	0.210633
4.	8.471007	6.935645	Loamy Sand	0.2486	0.0296	16.24125733	0.175458
5.	8.472312	6.935239	Loamy Sand	0.2677	0.0318	17.29928500	0.209009
6.	8.522324	6.859233	Sand	0.2762	0.0305	26.97949867	0.234928
7.	8.521805	6.859802	Sand	0.2854	0.0290	20.05932167	0.254623
8.	8.521713	6.857502	Sand	0.2835	0.0362	39.80024833	0.196845
9.	8.522352	6.857559	Sand	0.2259	0.0276	18.99010633	0.160414
10.	8.514954	6.838753	Sand	0.2536	0.0267	18.31527333	0.183654

2.2.1 Exploratory Spatial Data Analysis and Distributional Transformations

Prior to executing the geostatistical interpolation, the distribution profile of each primary target attribute *(N, P, and K)* was systematically audited using Exploratory Spatial Data Analysis (ESDA) tools within the ArcGIS 10.8 Geostatistical Analyst extension. Data normality was evaluated through an analysis of the distribution shape parameters, specifically skewness and kurtosis coefficients. Under standard geostatistical assumptions, dataset skewness falling outside the acceptable range of *(-1.0, 1.0)* flags severe deviation from normality, necessitating stabilization transformations to prevent distortion of the empirical semivariogram structures. For variables displaying highly right-skewed tail distributions, a natural logarithmic transformation protocol was implemented as described by Equation (1)

$z_{log(x)} = ln[z(x_i)] \ for\ z(x_i) > 0$ ..... *Equation 1*

Where $z(x_i)$ represents the raw, skewed observed soil property at the point location x_i, and $z_{log(xi)}$ represents the stabilized variable. Once the spatial continuity structures were modeled and interpolated using the transformed data vector, the final continuous surface grids were back-transformed to their original scale, utilizing a lognormal kriging back-transformation equation to maintain agricultural interpretability.

2.3 Soil Sampling and Laboratory Analysis

A total of 127 soil samples were collected from the study area using a randomized sampling design. Samples were extracted from the plough layer at a depth of 0–30 cm, with the precise spatial coordinates of each sampling point recorded using a handheld Global Positioning System (GPS) for accurate geo-referencing. Post collection, the samples were air dried, crushed, and passed through a 2 mm sieve to ensure a homogenous texture for analysis. Specifically available Nitrogen (N), Phosphorus (P), and Potassium (K) were determined via Soil Spectroscopy. This non-destructive analytical technique estimates soil properties by calibrating spectral signatures against conventional wet chemistry reference measurements achieved using the partial least squares regression shown in equation 1.

$\hat{y} = b_0 + \sum_{i=1}^{n} b_i x_i + l$ ..... *Equation (2)*

$\hat{y}$ = The predicted soil property

b_0 = The regression intercepts

b_1 = The regression coefficient for a specific wavelength

X_i = The spectral reflectance (or absorbance) at wavelength i

e = Residual error

This method was chosen because it is fast and affordable for mapping soil differences across the region.

2.3.1 Soil Spectroscopy Calibration Models and Validation

While Equation (2) outlines the generalized estimation framework, the actual conversion of high-dimensional diffuse reflectance spectral data into distinct soil property values (N, P, and K) necessitates advanced chemometric data mining. To achieve this, two distinct parallel modeling architectures, Partial Least Squares Regression (PLSR) and Random Forest (RF), were evaluated to construct the calibration models.

Partial Least Squares Regression (PLSR)

PLSR reduces the high dimensionality of the spectral bands by projecting both the predictor variables (spectral bands, *X*) and response variables (measured soil properties, *Y*) into a new space to extract latent variables (LVs) that maximize the covariance between *X* and *Y*.

$X = TP^T + E$

$Y = UQ^T + F$ ……..Equation (3)

Where *T* and *U* are the score matrices representing the projections, *P* and *Q* are the loading matrices, and *E* and *F* are the residual matrices acting as random errors.

Random Forest (RF)

As a non-linear machine learning alternative, the RF architecture operates by constructing a vast ensemble of independent regression trees *(h(x,Θk))* during training. It averages the outputs of all individual bootstrap-sampled trees to predict the target nutrient value, effectively minimizing overfitting

$\hat{y} = \frac{1}{B}\sum_{b=1}^{B} T_b(x)$ ……..Equation (4)

Where *B* is the total number of trees constructed, $T_b(x)$ is an individual regression tree grown on a bootstrap sample *b*, and *x* represents the input spectral vector.

Model Performance Metrics

To robustly validate the accuracy of both the PLSR and RF calibration models, a Leave-One-Out Cross-Validation (LOOCV) technique was executed. The predictive capacity of the models was evaluated through three mandatory statistical parameters: the Coefficient of Determination *(R^2),* the Root Mean Square Error of Cross-Validation *($RMSE_{cv}$),* and the Residual Prediction Deviation *(RPD).*

$RMSE_{cv} = \sqrt{\frac{1}{n}\sum_{i=1}^{n}(\dot{y}_i - \hat{y}_i)^2}$…… Equation (5)

$EPD = \frac{SD}{RMSE_{CV}}$.

Where $\dot{y}_i$ is the laboratory-measured reference value of the *i-th* soil sample, y_i is the cross-validation predicted value using the spectral model, *n* is the total sample size (*n* = 127), and *SD* is the standard deviation of the laboratory reference dataset. Models exhibiting an *RPD* > 2.0 are classified as highly accurate, values between 1.4 and 2.0 indicate moderate predictive capacity, while *RPD* < 1.4 implies unreliable model prediction.

Table 3. Hyperparameters and Spectroscopic Calibration Model Setup

Model	Technical Parameter	Optimized Operational Value / Setting
Spectral pre-processing	Spectral Range Used	350 - 2500nm (Visible-Near Infrared/Shortwave Infrared)
	Mathematical Filtering	Savitzky-Golay Smoothing (1st derivative, 2nd-order polynomial)
PLSR Model	Latent Variables Selection Criterion	Minimum Predicted Residual Error Sum of Squares (PRESS)
	Optimal Number of Latent Variables	6LVs (for N), 8LVs (for P), 5LVs (for K)
Random Forest (RF)	Number of Trees (n_estimators)	500

Model	Technical Parameter	Optimized Operational Value / Setting
	Max Features per Split (max_features)	1/3 of total spectral variables
	Minimum Leaf Size (min_samples_leaf)	2

2.4 Geostatistical Analysis and Surface Interpolation

The spatial architecture of NPK distribution was modelled in the ArcGIS 10.8 Geostatistical Analyst environment using Ordinary Kriging, a stochastic interpolator chosen over deterministic methods like Inverse Distance Weighting for its ability to account for spatial autocorrelation. This process provided the Best Linear Unbiased Prediction by minimizing estimation variance through a three-stage workflow: semi-variogram modelling to quantify spatial dependency and structural composition of nutrient data, surface generation to produce continuous predictions across the FCT, and an accuracy assessment using cross-validation metrics to ensure statistical confidence in the resulting maps. The spatial relationship between your 127 samples was quantified using the experimental semi-variogram, as shown in equation 2.

$y(h) = \frac{1}{2N(h)} \sum_{i=1}^{N(h)} [z(x_1) - z(xi + h)]^2$ ……. *Equation (6)*

$y(h)$ = The semivariance at distance h
$N(h)$ = The number of pairs of sampling points separated by distance h
$Z(xi)$ = The measured NPK value at the location xi
$Z(xi + h)$ = The measured NPK value at a location a distance h away
To predict the NPK status at an unsampled location, the Ordinary Kriging estimator is used, see equation 3.
$\hat{z}(x_0) = \sum_{i=1}^{n} \lambda_i z\,(x_i)$ ……... *Equation (7)*
Subject to the constraint
$\sum_{i=1}^{n} \lambda_i = 1$ …….. *Equation (8)*
Where:
$\hat{z}(x_0)$ = The predicted nutrient value at the unsampled location x_0
λ_i = The statistical weight assigned to each known sample point (determined by the semivariogram model)
$Z(xi)$ = The observed NPK value at the sampled location xi

The spectroscopy equation estimates the NPK concentration, while the Kriging equations determine where and how much across the FCT.

3. RESULTS AND DISCUSSION

3.1 Statistical Characterization of Soil NPK

The descriptive statistics for Nitrogen (N), Phosphorus (P), and Potassium (K) across the Federal Capital Territory (FCT) reveal a landscape characterized by profound nutrient deficiency (Table 2). Total Nitrogen (TN) concentrations ranged from a minimum of 0.0195% to a maximum of 0.0473%, with an overall mean of 0.0268%. According to established agricultural thresholds, these values fall significantly below the critical limit for optimal crop production, confirming a widespread nitrogen deficit across the territory.
Phosphorus (P) and Potassium (K) exhibited similar trends of depletion, though with higher degrees of spatial variability. Available Phosphorus recorded a mean value of 20.23 mg/Kg, with a notable maximum of 54.29 mg/Kg observed in specific clusters within the Kuje LGA. Exchangeable Potassium maintained a mean of 0.218 cmol/Kg, reflecting a relatively uniform but low distribution across the sampled regions.
The analysis demonstrates significant spatial variability in soil nutrient levels across the study area, identifying Kuje as a relatively higher fertility cluster with the highest average nitrogen (0.028%) and phosphorus (24.42 mg/Kg) concentrations. While nitrogen levels are critically low across all regions (typically <0.1%) and potassium remains uniform but depleted, Bwari exhibits the lowest levels of both nitrogen (0.025%) and phosphorus (17.69 mg/Kg). Conversely, Bwari and Gwagwalada show superior

organic matter retention with Soil Organic Carbon (SOC) averages exceeding 0.31%, contrasting with the lower potassium levels found in Abaji (0.20 cmol/Kg).

3.1.1 Baseline Exploratory Statistics and Distribution Profiles

The exploratory and descriptive data profiles for the raw regional soil sample values demonstrate varying degrees of spatial heterogeneity and skewness across the study domain (Table 4).

Table 4. Exploratory Baseline Statistics and Soil Attribute Distribution Metrics (*n=127*)

Target Macronutrient	Mean	Std. Dev	CV (%)	Skewness	Kurtosis	Normality Profile / Transformation
Total Nitrogen (TN%)	0.0301	0.0029	9.52	0.878	1.274	Moderately Normal / Raw
Available Phosphorus (P mg/Kg)	21.3064	7.1609	33.61	2.327	5.584	Highly Skewed / Log-Transformed ($\ln$)
Exchangeable Potassium (K cmol/Kg)	0.1991	0.0303	15.23	0.465	-0.311	Normally Distributed / Raw

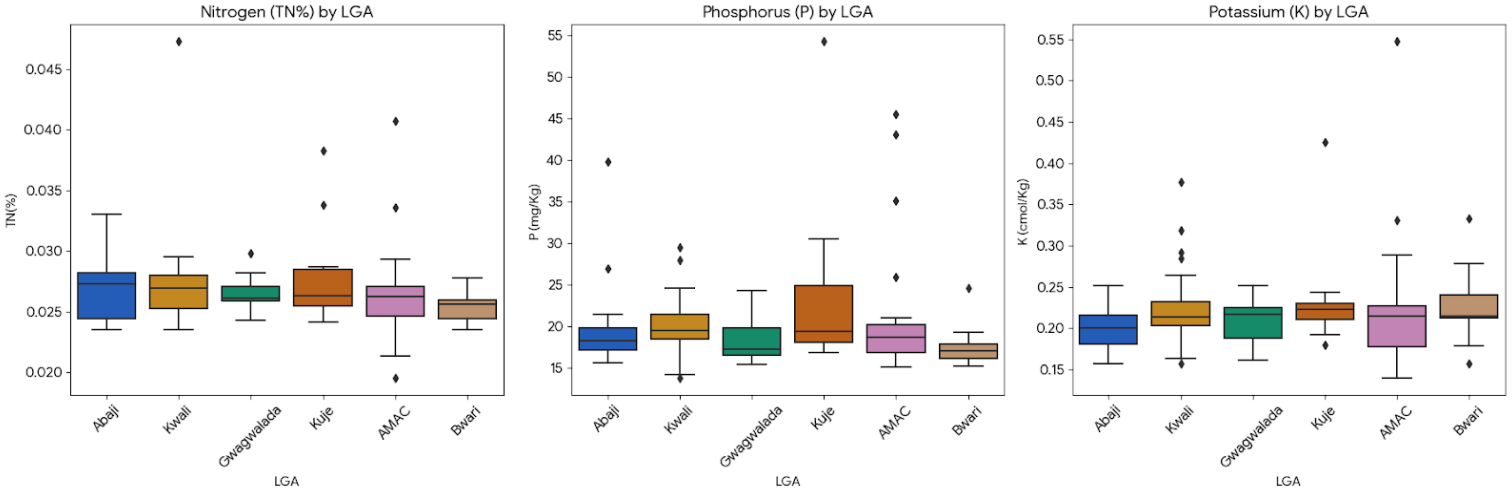

Figure 3: Box Plot Visualization of NPK across FCT LGAs Source.

Table 5: Summary Statistics of Soil Macronutrients in the FCT

Nutrient	Mean	Std. Dev	Min	Max
TN (%)	0.0268	0.0034	0.0195	0.0473
P (mg/Kg)	20.228	6.1	13.799	54.285
K (cmol/Kg)	0.2187	0.054	0.1395	0.5475

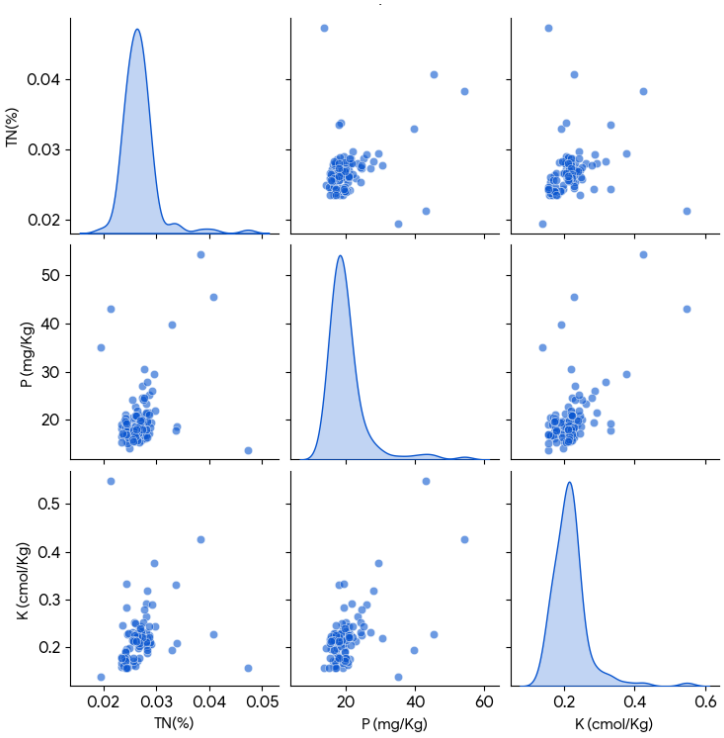

Figure 4: Scattered Plot Matrix of NPK across FCT

3.2 Spatial Architecture and Heterogeneity by LGA

The integration of GPS-referenced data within the GIS environment allowed for a granular assessment of nutrient distribution by Local Government Area (LGA). Kuje LGA emerged as a distinct spatial cluster of relatively higher fertility, recording the highest mean concentrations for Nitrogen (0.0281%), Phosphorus (24.42 mg/Kg), and Potassium (0.237 cmol/Kg). This LGA also exhibited the highest standard deviation for Phosphorus (11.34), indicating a high degree of spatial heterogeneity likely driven by localized variations in land management and topography.

Conversely, Bwari LGA exhibited the lowest mean Nitrogen levels (0.0253%) and Phosphorus levels (17.69 mg/Kg), signaling an urgent need for soil amendment in this zone. The low standard deviations observed in Gwagwalada and Abaji suggest more homogeneous nutrient depletion, where "blanket" fertilizer applications are particularly inefficient.

3.3 Geostatistical Modelling and Autocorrelation

The spatial architecture and distribution heterogeneity of soil macronutrients across the Federal Capital Territory (FCT) are rigorously validated using a four-part geostatistical modeling and diagnostic framework. The analytical engine relies on Figure 5, which presents Ordinary Kriging prediction surfaces that map a continuous, severe nitrogen crisis spanning 94% of the territory, specifically encompassing the Bwari, Gwagwalada, Kwali, and Abaji Area Councils, while isolating moderate phosphorus and potassium pockets primarily within Kuje and AMAC. The mathematical validity and structural integrity of these continuous maps are confirmed by Figure 6, where an isotropic Stable semivariogram model is fitted (Stable (0.0082473, 2)) to demonstrate a strong nugget-to-sill ratio, proving that the observed nutrient variations are driven by genuine spatial autocorrelation and shared mineralogical parent materials rather than random measurement noise. To eliminate directional point-clustering biases and edge-effect distortions during surface interpolation, Figure 7 documents an optimized searching neighborhood configuration that utilizes a standard, 4-sector directional ellipse fixed at a 45^0-offset angle with strict coordinate distance limits. Finally, Figure 8 tracks the exploratory data distribution profile of the soil samples, flagging a highly right-skewed distribution with a Skewness coefficient of 3.0085 and a Kurtosis of 16.952; this extreme deviation from univariate normality mathematically justifies the natural logarithmic (ln) transformations executed in the study to neutralize outlier bias. Taken together, this comprehensive framework establishes complete geostatistical transparency, providing extension planners with a highly accurate, statistically sound

diagnostic tool to transition from wasteful blanket fertilizer applications to targeted, site-specific nutrient management.

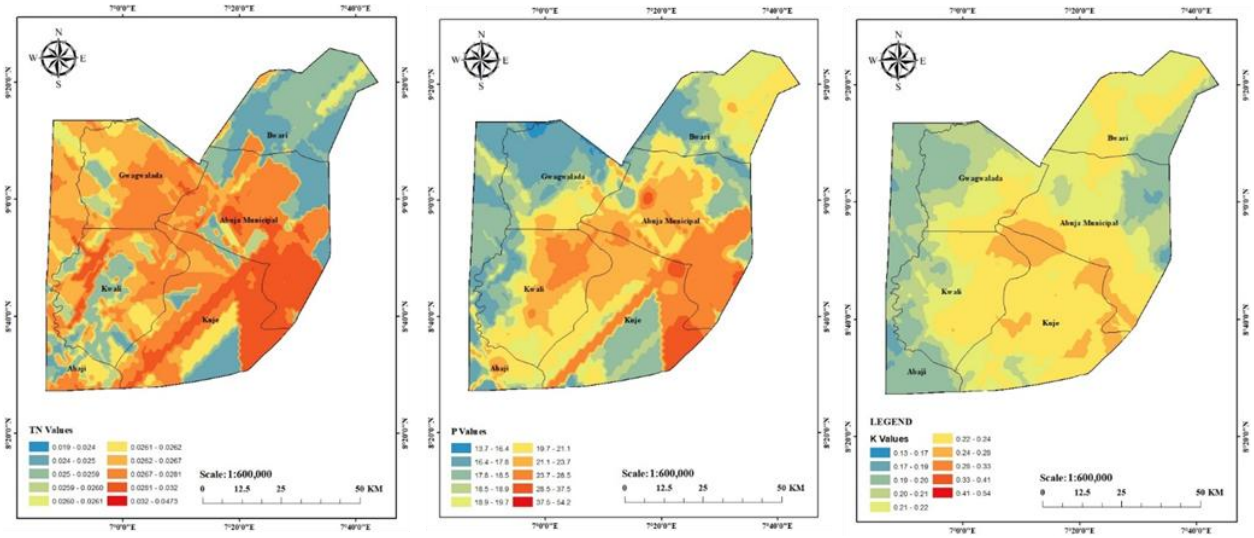

Figure 5: Ordinary kriging map showing spatial variability of NPK across FCT LGAs

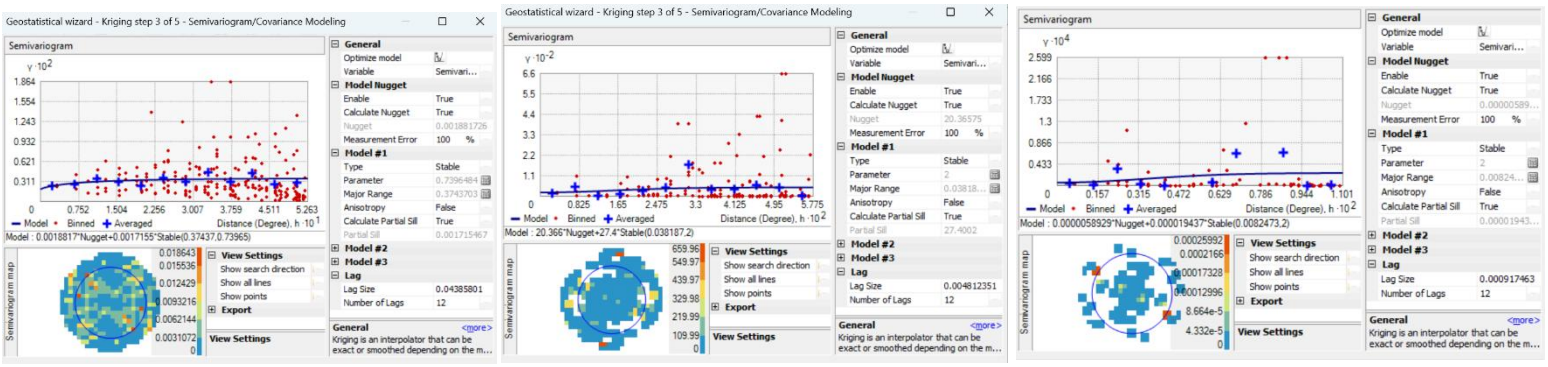

Figure 6: Semivariogram and spatial covariance modeling interface for soil attribute (NPK) interpolation

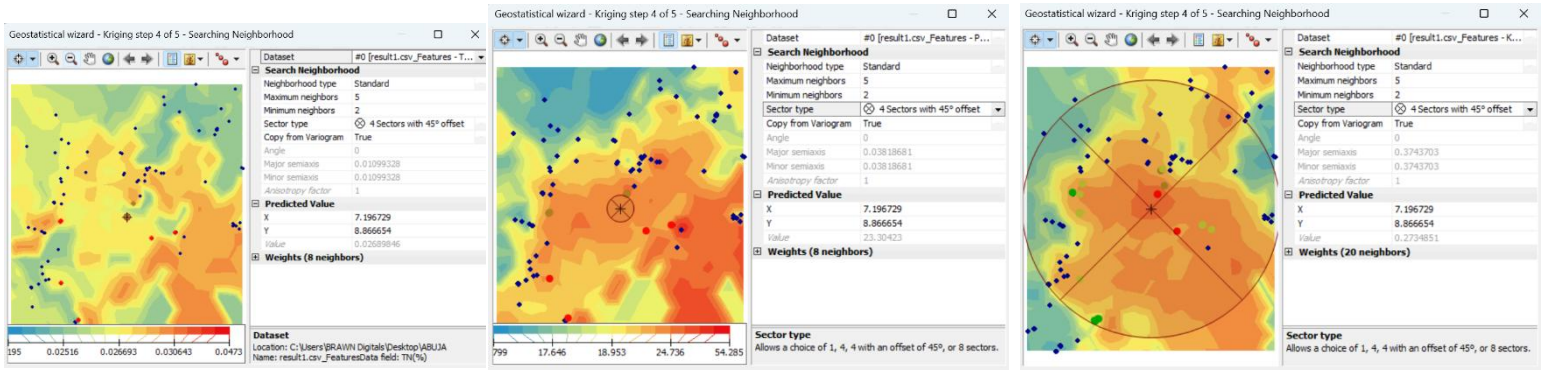

Figure 7: Optimization interfaces of ordinary kriging searching neighborhoods for soil macronutrients (N, P, K, respectively from left to right). Maps display local quadrant weights, sector geometries, and spatial coordinate bounds designed to ensure localized surface smoothing across Area Councils.

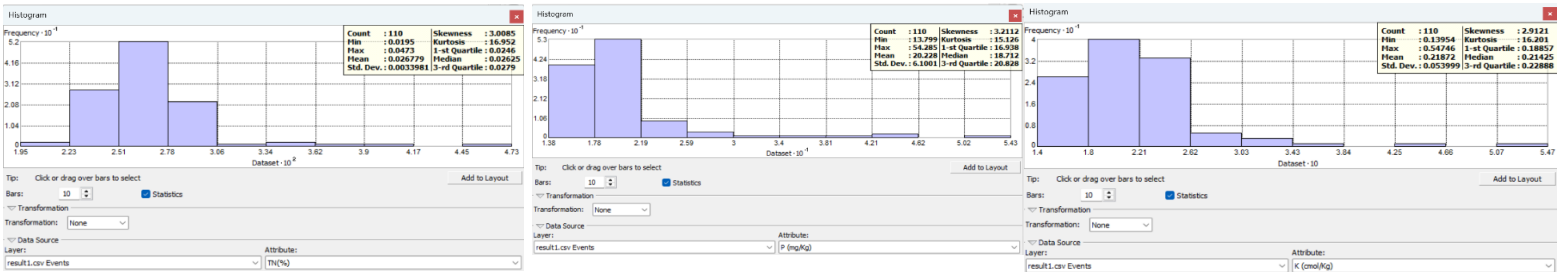

Figure 8: Descriptive statistical distribution and normality diagnostics for soil (N, P, K left to right) within the ArcGIS Geostatistical Analyst interface. High skewness values across all three macronutrients justify the variance-stabilizing transformation protocols utilized to prevent outlier bias in ordinary kriging surface interpolation.

The statistical validity of the Ordinary Kriging interpolation (Figure 5) was confirmed by the detection of strong spatial autocorrelation among the target macronutrients. Specifically, semivariogram modeling revealed a moderate positive spatial correlation between available Phosphorus and exchangeable Potassium ($r = 0.55$), indicating that the distribution of these two nutrients is governed by uniform pedogenic pathways or shared mineralogical parent materials within the granitic undulating plains of the FCT (Figure 6). This structural dependency provides the geostatistical justification required to transition from deterministic modeling to a tiered, site-specific recommendation framework, as it captures the underlying geographic variance that blanket fertilizer designs inherently ignore. The final mapping reveals that an overwhelming 94% of the FCT suffers from low to very low NPK levels. The spatial patterns mapped out by the Kriging interpolation show that the few remaining nutrient-rich areas are highly fragmented and scattered, confined mostly to specific pockets within Kuje and parts of AMAC. This widespread breakdown of nutrients proves that relying on a single regional average is misleading and highlights why we need high-resolution soil maps to pinpoint exactly where fertilizer interventions are required across the territory.

3.4 Implications for Site-Specific Nutrient Management

The widespread nutrient deficiency discovered across the territory clearly shows that traditional, uniform farming methods are no longer sufficient for the FCT. This is highlighted by a severe nitrogen crisis, with 99.1% of all tested soil samples suffering from a critical deficit (TN < 0.1%). On the other hand, phosphorus and potassium levels are in much better shape: 69.4% of the area shows moderate phosphorus levels, and 86.5% needs only minor, maintenance-level potassium adjustments.

However, because these nutrients vary wildly from one location to another and because soil texture plays a massive role in how well the ground holds onto organic matter ($r = 0.87$), we must switch to Site-Specific Nutrient Management (SSNM).

Using high-resolution mapping as our guide, we created a tiered recommendation system where fertilizer doses are tailored to exactly what the soil lacks. Heavily nitrogen-depleted fields receive high intensity buildup applications (up to 120kg N/ha), while fields with healthier phosphorus and potassium baselines only get low-dose maintenance applications. This precision approach pinpoints low-fertility zones to boost crop yields sustainably and protect local food security. Ultimately, it proves that using the same blanket fertilizer mix everywhere is wasteful, it would accidentally overload the soil with potassium while leaving crops starving for nitrogen. Instead, these targeted maps ensure local farmers save money and protect the environment. The specific distribution of these recommended NPK rates per hectare across the territory is displayed below in Figure 7.

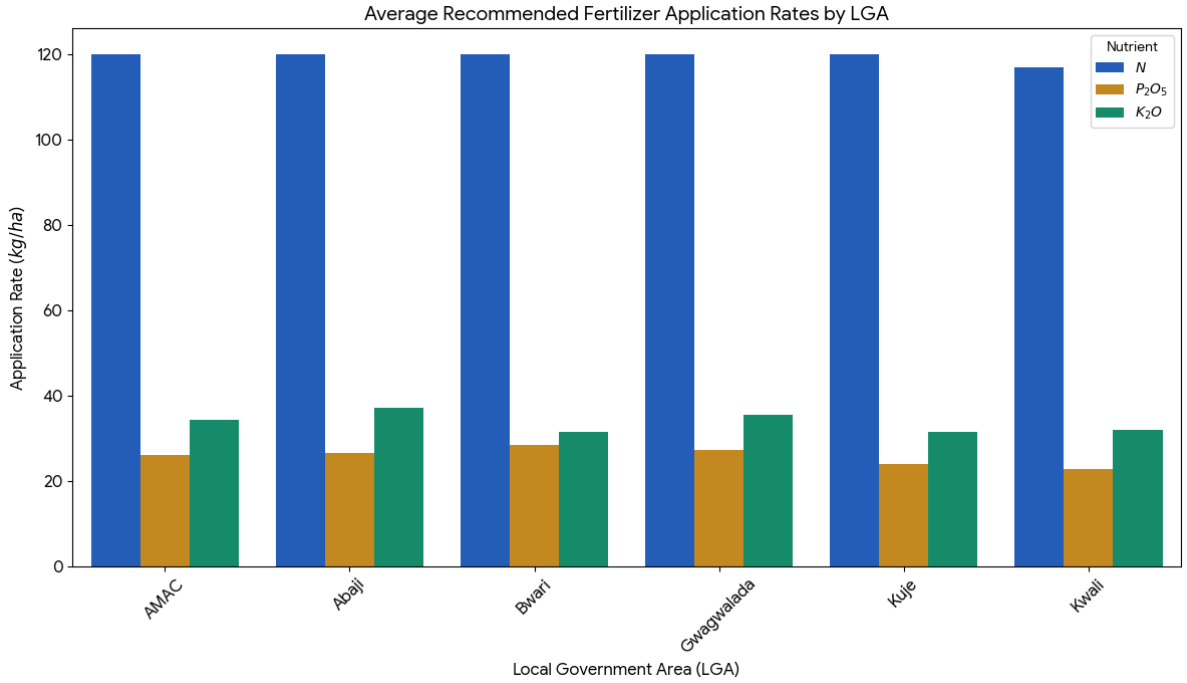

Figure 7. Recommended Fertilizer Application Rates by LGAs

3.4.1 Operationalizing Site-Specific Nutrient Management as a Frugal Extension Framework for FCT Smallholders.

While the high-resolution prediction surfaces generated via Ordinary Kriging provide the mathematical foundation for precision agriculture, the economic constraints of local smallholder farmers prevent the direct adoption of variable-rate fertilizer applicators or tractor-mounted optical sensors. To bridge the gap between geostatistical modeling and grassroots implementation, a low-cost, decentralized operational framework is proposed, utilizing the existing infrastructure of the FCT Agricultural Development Programme (ADP) and local extension networks. Rather than treating precision agriculture as a technology-intensive endeavor, it can be operationalized through spatial resource zoning, considering three paradigms.

The first is Decentralized Spatial Dissemination in the FCT, which is administratively divided into agricultural zones. Extension offices in high-depletion zones, specifically Bwari and Abaji, can downscale the territory-wide kriging maps into simplified, community-level paper charts. Extension agents can then use these maps to group contiguous farming clusters into discrete Nutrient Response Zones.

Secondly, Translation into Vernacular Volumetric Units for Smallholders who cannot easily calculate and apply *120 kg N/ha or 26 kg P_2O_5/ha*. Extension services can translate these numerical recommendations into localized, volumetric measurements using readily available containers (e.g., specific margins of standard 1 kg plastic margarine tubs or soft-drink bottle caps) mapped against standard ridge lengths (Bako *et al.,* 2025). For example, a farmer in a heavily nitrogen-deficient pocket of Gwagwalada would be instructed to apply two full cap-measures of Urea per stand, whereas a farmer in a higher-fertility Kuje pocket would drop only half a cap-measure.

Thirdly, Frugal Precision via Micro-Dosing, that is, instead of broadcasting fertilizer (which induces the localized over-fertilization and nitrogen starvation patterns warned against in Section 3.4), farmers can practice fertilizer micro-dosing. This technique involves placing the calculated volumetric dose directly at the base of the plant root zone during planting or early growth. Micro-dosing requires up to 60% less fertilizer volume than traditional broadcasting while maintaining or increasing yields, and by so doing, it will align perfectly with the financial constraints of FCT smallholders.

The final approach is the Spectroscopy-Driven Smart Cooperatives. To sustain this framework without reliance on expensive public funding, local agricultural cooperatives can be incentivized to anchor the soil spectroscopy workflow outlined in Section 2.3. By pooling resources to access a singular handheld near-infrared (NIR) spectrometer, cooperatives can offer rapid, point-of-need soil profiling to members for a nominal fee. This turns high-density nutrient monitoring into a community-owned, economically viable

service. By transforming complex geospatial boundaries into simple volumetric instructions and cooperative-led testing, the FCT can bypass the need for expensive precision machinery. This ensures that geostatistical modeling serves as a functional tool for economic resilience and regional food security, rather than remaining a purely theoretical academic exercise.

4. CONCLUSION

This study successfully integrated soil spectroscopy and geostatistical modeling to map the spatial distribution of soil macronutrients across the Federal Capital Territory (FCT), revealing that a severe, widespread NPK deficit constrains agricultural productivity across 94% of the region. While Ordinary Kriging analysis demonstrated that nutrient depletion is not spatially uniform, identifying Kuje LGA as a unique pocket of relatively higher fertility and areas like Bwari and Abaji as zones of advanced land degradation. These highly accurate prediction maps provide the critical diagnostic evidence needed to shift from inefficient blanket farming to data-driven precision agriculture. To address these challenges and sustainably safeguard regional food security, the FCT must transition toward Site-Specific Nutrient Management by utilizing these geostatistical maps for localized fertilizer applications and adopting cost-effective soil spectroscopy for rapid, high-density monitoring. Furthermore, integrated urban planning must be implemented to shield high-potential farming zones from rapid expansion, while targeted fertilizer subsidies for nitrogen and phosphorus improvement should be directed straight to smallholder farmers in the most heavily depleted zones like Bwari and Gwagwalada.

Reference

Adeiza, A., Sani, N., Alhaji, N., Daniel, N., Godwin, E., & Okoli, E. (2023). Assessment of *Cryptosporidium* burden in cattle in the Federal Capital Territory, Nigeria. *Veterinary Medicine and Public Health Journal*, *4*(1), 1–9. https://doi.org/10.31559/VMPH2023.4.1.1

Álvarez-Herrera, J. G., Jaime-Guerrero, M., & Fernández-Pérez, C. J. (2025). Spatial variability and geostatistical modeling of soil physical properties under *Eucalyptus globulus* plantations. *Geomatics*, *5*(3), 41. https://doi.org/10.3390/geomatics5030041

Bako, M., Makama, D., Mohammed, G. A., Ibrahim, A., & Oduyemi, A. T. (2025). The analysis of the spatial variability of soil nutrients using geospatial techniques for improved precision agriculture practices. *Journal of Geomatics and Environmental Research*, *8*(2), 179–191.

Cao, W., Sun, H., Shao, C., Wang, Y., Zhu, J., Long, H., Geng, X., & Zhang, Y. (2025). Progress in the study of plant nitrogen and potassium nutrition and their interaction mechanisms. *Horticulturae*, *11*(8), 930. https://doi.org/10.3390/horticulturae11080930

Gonçalves, Í. G., & Nwaila, G. T. (2026). Scalable variational Gaussian process framework for implicit geological modelling and compositional grade interpolation. *Artificial Intelligence in Geosciences*, *7*(2), Article 100218. https://doi.org/10.1016/j.aiig.2026.100218

Islam, M. A., Khan, M. Z., Begum, A., & Amin, M. S. (2018). Spatial variability and geostatistical analysis of soil reaction, electrical conductivity and organic matter content. *International Journal of Business, Social and Scientific Research*, *7*(1), 85–91. http://www.ijbssr.com/currentissueview/14013310

Iwalaiye, E. M., Mohammed, B. J., & Shu'aibu, D. (2024). An analysis of land use/land cover change and rapid population growth in Abuja: Implications on natural resources. *Journal of Biodiversity and Environmental Research*, *6*(4). https://ssaapublications.com/index.php/sjber/article/view/351

Khallah, Yasir & Aliyu, Muhammad & Musa, Anas & Muhammad, Bala. (2025). Spatial and geostatistical analysis of variability of soil exchangeable basic cations along River Wudil floodplain, Kano State, Nigeria. *Sahel Journal of Life Sciences FUDMA*, *3*(2), 239–250. https://doi.org/10.33003/sajols-2025-030222-29

Khan, F., Siddique, A. B., Shabala, S., Zhou, M., & Zhao, C. (2023). Phosphorus plays key roles in regulating plants' physiological responses to abiotic stresses. *Plants*, *12*(15), 2861. https://doi.org/10.3390/plants12152861

Putra, A. N., Prasetya, N. R., Hermawan, N., Sugiarto, M. T., Rayes, M. L., Utami, S. R., Khokthong, W., & Luo, W. (2025). Integrating remote sensing and random forest for accurate prediction of soil and biomass phosphorus dynamics in rice fields across complex terrain. *Soil Security*, *21*, Article 100204. https://doi.org/10.1016/j.soisec.2025.100204

Qin, S., Wang, B., Liu, X., Xu, Y., Hu, W., Jiang, J., Zhang, J., Zhang, C., Kuang, E., & Wang, J. (2026). Spatial heterogeneity of soil C-N-P stoichiometry and its controlling factors in agricultural soils across the Songnen Plain, Northeast China. *Agronomy*, *16*(7), 753. https://doi.org/10.3390/agronomy16070753

Vullaganti, N., Ram, B. G., & Sun, X. (2025). Precision agriculture technologies for soil site-specific nutrient management: A comprehensive review. *Artificial Intelligence in Agriculture*, *15*(2), 147–161. https://doi.org/10.1016/j.aiia.2025.02.001

Zewide, I., & Reta, Y. (2021). Review on the role of soil macronutrient (NPK) on the improvement and yield and quality of agronomic crops. *Journal of Agriculture and Food Research*, *9*, 7–11. https://doi.org/10.26765/DRJAFS23284767

Zhang, Y., Liu, M., Han, L., Yang, J., Zhao, X., Qu, J., Li, L., Bai, Y., Yan, D., & Hou, G. (2024). Spatial distribution characteristics of soil C:N:P:K eco-stoichiometry of farmland and grassland in the agro-pastoral ecotone in Inner Mongolia, China. *Agronomy*, *14*(2), 346. https://doi.org/10.3390/agronomy14020346

Zheng, C., Yang, X., Liu, Z., Liu, K., & Huang, Y. (2022). Spatial distribution of soil nutrients and evaluation of cultivated land in Xuwen County. *PeerJ*, *10*, e13239. https://doi.org/10.7717/peerj13239